N73-24929
NASA TM X-2791

NASA TECHNICAL MEMORANDUM

NASA TM X-2791

ENGINE INVESTIGATION OF AN IMPINGEMENT-COOLED TURBINE ROTOR BLADE

by James W. Gauntner and John N. B. Livingood

Lewis Research Center
Cleveland, Ohio 44135

NATIONAL AERONAUTICS AND SPACE ADMINISTRATION • WASHINGTON, D. C. • MAY 1973

1. Report No.	2. Government Accession No.	3. Recipient's Catalog No.
NASA TM X-2791		

4. Title and Subtitle	5. Report Date
ENGINE INVESTIGATION OF AN IMPINGEMENT-COOLED TURBINE ROTOR BLADE	May 1973
	6. Performing Organization Code

7. Author(s)	8. Performing Organization Report No.
James W. Gauntner and John N. B. Livingood	E-7313
	10. Work Unit No. 501-24

9. Performing Organization Name and Address	11. Contract or Grant No.
Lewis Research Center National Aeronautics and Space Administration Cleveland, Ohio 44135	
	13. Type of Report and Period Covered
12. Sponsoring Agency Name and Address	Technical Memorandum
National Aeronautics and Space Administration Washington, D.C. 20546	14. Sponsoring Agency Code

15. Supplementary Notes

16. Abstract

Experimentally determined heat-transfer characteristics of an impingement-cooled turbine rotor blade are reported. The test results are compared with results obtained for three convection-cooled turbine blades tested in the same facility and with impingement correlations found in the literature.

17. Key Words (Suggested by Author(s))	18. Distribution Statement
Turbine blade Impingement cooling Heat transfer	Unclassified - unlimited

19. Security Classif. (of this report)	20. Security Classif. (of this page)	21. No. of Pages	22. Price*
Unclassified	Unclassified	22	$3.00

* For sale by the National Technical Information Service, Springfield, Virginia 22151

ENGINE INVESTIGATION OF AN IMPINGEMENT-COOLED TURBINE ROTOR BLADE

by James W. Gauntner and John N. B. Livingood

Lewis Research Center

SUMMARY

The heat-transfer characteristics of an impingement-cooled turbine rotor blade were determined experimentally. The blade was tested in a modified turbojet engine capable of operating at average turbine-inlet temperatures to 1644 K (2500° F). The experimental results obtained for the impingement-cooled blade are compared with those of three convection-cooled blades (a chordwise-passage blade, a spanwise-passage blade, and a simple cast blade) previously tested in the same engine.

Over the range of engine operating conditions considered, it was found that the impingement-cooled blade was cooled more effectively than were the other three blades. For a given turbine-inlet temperature, coolant temperature, and coolant-to-gas flow ratio, the maximum blade temperature and the difference between maximum and minimum chordwise blade temperatures at the midspan were less for the impingement blade than for the other three blades. One of these three blades had a lower average temperature but also had a less uniform temperature distribution. For the same coolant temperature, coolant-to-gas flow ratio, and a maximum blade temperature of 1255 K (1800° F), the allowable turbine-inlet temperature was higher for the impingement blade than for the other three blades.

Experimental midspan blade temperatures and midspan Nusselt numbers were compared with predicted values. Nusselt number correlations from the literature generally agreed with data from the leading edge and the midchord regions of the impingement-cooled blade. Crossflow did not appear to affect impingement heat transfer in the midchord region.

INTRODUCTION

An experimental investigation was made to determine the heat-transfer characteristics of an impingement-air-cooled turbine blade. The results of this investigation

were used to compare measured blade temperatures with calculated design wall temperatures, to compare the cooling capabilities of the blade with the cooling capabilities of blades of other cooling configurations previously tested, and to compare wall-to-coolant Nusselt numbers calculated from the data with those calculated from correlations in the literature.

The impingement-cooled blade seemed attractive because of its anticipated efficient cooling and because of its relative ease of fabrication. References 1 and 2 reported the results for the convection-cooled blades mentioned above. Reference 1 reported the results of tests on a chordwise-finned blade with an impingement-cooled leading edge and a slotted trailing edge. Reference 2 reported test results for a spanwise-finned blade with an impingement-cooled leading edge and a slotted trailing edge and for a simple cast blade with radial coolant passages discharging at the blade tip. The blade of reference 1 and the spanwise-finned blade of reference 2, as well as the one investigated herein, were designed and fabricated at the NASA Lewis Research Center.

The blades were tested in a modified J75 turbojet engine capable of operating at average turbine-inlet temperatures to 1644 K (2500° F). The research engine is described in reference 3. Test conditions for the impingement blades covered the following ranges of variables: turbine-inlet temperatures from 1367 to 1644 K (2000° to 2500° F); cooling-air-inlet temperatures of 300, 589, and 811 K (80°, 600°, and 1000° F); turbine-inlet pressures from about 22 to 28 newtons per square centimeter absolute (32 to 41 psia); and coolant flow ratios to about 10 percent.

SYMBOLS

A coefficient in eq. (1)

B exponent of $(\dot{w}_c/\dot{w}_g)$ in eq. (1)

D diameter of leading edge of blade

h heat-transfer coefficient

k thermal conductivity

L length of blade surface measured from stagnation point

Nu Nusselt number

P total pressure

Pr Prandtl number

p static pressure

Re Reynolds number

r distance along span measured from blade hub

S heat-transfer surface area

T temperature

$\dot{w}$ flow rate

x chordwise distance along blade surface from stagnation point

θ angle measured from stagnation point

φ temperature-difference ratio (eq. (2))

Subscripts:

b based on equivalent slot width

c coolant or coolant side

c, i coolant inlet

g gas or gas side

ge effective gas

max maximum midspan

min minimum midspan

p pressure surface

r, i relative inlet

s suction surface

t, i turbine inlet

w wall

x based on nozzle diameter of midchord jets

Superscript:

$\bar{}$ average

TEST BLADE

The impingement blade consisted of a structure-bearing outer shell with an insert as shown in figures 1 and 2. The outer shell was tapered both in cross section and in shell thickness from hub to tip. The insert formed a 0.025-centimeter- (0.010-in.-) thick sheet-metal plenum with 543 hole perforations. Cooling at the leading edge and in the midchord region was provided by air impinging on the outer shell through the insert

perforations. The trailing edge was cooled by means of thin chordwise slots. The impingement-cooling air, after impingement, flowed chordwise along the blade suction and pressure surfaces between the outer and inner shells and was exhausted through the trailing-edge slots. These slots were designed to be flow constraints. The blade had a 10.2-centimeter (4.0-in.) span and a midspan chord of 4.1 centimeters (1.6 in.). Figure 1(a) shows the slotted trailing edge of the impingement-cooled blade.

Along the leading-edge region of the insert was a row of 92 holes, each 0.064 centimeter (0.025 in.) in diameter. The center-to-center spacing of these holes was 0.081 centimeter (0.032 in.) in the hub section, 0.108 centimeter (0.043 in.) in the central section, and 0.155 centimeter (0.061 in.) in the tip section. These leading-edge holes were spaced 5 nozzle diameters from the point of impingement at the midspan. A total of 451 holes, each 0.030 centimeter (0.012 in.) in diameter, were provided in the midchord region of the blade; 277 of these holes were on the suction side, and 174 on the pressure side of the perforated insert. Spacings of these holes varied with both spanwise and chordwise position. These midchord holes were spaced 2.5 nozzle diameters from the blade outer shell. Figure 1(b) shows the relative locations of these holes.

The design geometries of the trailing edge slots were as follows: the hub section had three slots, each 0.081 centimeter by 0.655 centimeter (0.032 in. by 0.258 in.), spaced 0.157 centimeter (0.062 in.) edge to edge; the center section had 10 slots, each 0.081 centimeter by 0.330 centimeter (0.032 in. by 0.130 in.), spaced 0.157 centimeter (0.062 in.) edge to edge; and the tip section had eight slots, each 0.081 centimeter by 0.140 centimeter (0.032 in. by 0.55 in.), spaced 0.165 centimeter (0.065 in.) edge to edge. A later modification to the design resulted in omitting three of the land areas to get proper flow distribution. The second, fifth, and eighth lands from the tip region were omitted, and the actual trailing-edge slots were as shown in figure 1(a).

The largest flow quantity per unit length of trailing edge was provided for the quarter of the blade span nearest the hub. The central half of the blade span and the quarter of the blade span nearest the tip constituted the other blade sections. The coolant flow-rate distribution for these three sections was obtained by varying the area of the choked trailing-edge passages. The design coolant flow for each of the three sections was 33, 50, and 17 percent, respectively, of the total coolant flow per blade.

INSTRUMENTATION

The normal complement of operational instrumentation was used on the research engine. In addition, the following research instrumentation was used to measure conditions of specific interest.

Gas and Coolant Instrumentation

Eight actuating thermocouple probes were located at various circumferential positions ahead of the stator vanes to measure the turbine-inlet temperature. Each of these probes was activated to traverse radially across the gas stream to provide temperatures at nine equally spaced spanwise locations to determine a representative radial profile of the turbine-inlet temperature. Since the data of this report were for the midspan of the blade, the average turbine-inlet temperature was determined by averaging the middle three positions of the representative radial profile.

Originally, the coolant flow rate to the test blade proper was to be determined by using a venturi-measured flow rate in the supply line external to the engine and correcting it for leakage at the labyrinth seal system and at the blade base serrations. During testing, however, it was found that uncertainties in coolant flow rates due to leakages under rotating conditions resulted in unreliable blade coolant flow rates. Consequently, the test-blade coolant flow rate was calculated by the method of reference 1.

The temperature and static pressure of the test-blade cooling air were measured immediately before the coolant entered the rotating turbine disk. The cooling-air temperature was also measured at the base of the rotor blades just prior to entering the blade cooling passage. The coolant temperature at this location is hereinafter referred to as the coolant-inlet temperature.

Blade Instrumentation

Five adjacent blades in the 76-blade engine rotor were the impingement-cooled test blades. In order to obtain a satisfactory number of experimental wall temperatures, it was necessary to instrument all the test blades. Figure 2 shows the five adjacent test blades and the thermocouple locations on each blade. The figure shows that blade 1 had four thermocouples at the 5.08-centimeter (2.0-in.) span section and one thermocouple at the 3.81-centimeter (1.5-in.) section; blade 5 had four thermocouples at the 1.27-centimeter (0.5-in.) section; and blades 2, 3, and 4 had a total of 16 thermocouples at the 3.81-centimeter (1.5-in.) section. The exact locations of the thermocouples are given in table I.

The thermocouples were all sheathed thermocouples consisting of Chromel-Alumel thermoelements and magnesium oxide insulation in a 0.051-centimeter (0.020-in.) outside diameter Inconel 600 tube and were installed in radial grooves machined in the blade surface. All the thermocouples were formed with a closed and grounded hot junction. The forming and installation techniques are discussed in reference 4.

EXPERIMENTAL PROCEDURE

The instrumented five-blade test pack was installed in the turbine rotor, and the engine was operated over a range of average turbine-inlet temperatures from 1367 to 1644 K (2000° to 2500° F). The engine speed was varied from 7500 to 8700 rpm. Turbine-blade cooling-air inlet temperatures of 300, 589, and 811 K (80°, 600°, and 1000° F) were used. For each series of tests, a change of coolant flow rate was the primary variable. Table II summarizes the average engine operating conditions for each series of test points.

Usually, about 10 test points were taken for each series of runs. The first was obtained for a relatively large coolant flow rate; the others were then obtained by reducing the coolant flow rate in a stepwise manner. This procedure was stopped when a maximum blade-metal temperature of about 1200 K (1700° F) was reached. This value was believed to be the maximum safe operating temperature for the test blades from consideration of the stress-rupture characteristics of the blade material and of the weld joints.

ANALYSIS METHODS

A simplified method for correlating experimental vane- or blade-metal temperature data was developed in reference 5 and was used in references 1 and 2. This equation

$$\frac{1 - \varphi}{\varphi} = A\left(\frac{\dot{w}_c}{\dot{w}_g}\right)^B \tag{1}$$

is also used in the present report. The quantity φ is defined as

$$\varphi = \frac{T_{ge} - T_w}{T_{ge} - T_c} \tag{2}$$

To evaluate φ, the cooling-air temperature measured at the inlet to the blade base was used as T_c, and the midspan turbine-inlet relative temperature $T_{r,i}$ was used as the effective gas temperature T_{ge} at the midspan section. This relative temperature was obtained by correcting the measured average midspan turbine-inlet temperature $T_{t,i}$ for the effects of stator vane cooling-air dilution and turbine rotation. The correction consists of a 0.9 factor applied to the $T_{t,i}$ to obtain T_{ge} (ref. 2). The coolant flow and the gas flow per blade were used to evaluate $\dot{w}_c/\dot{w}_g$.

An alternate way of expressing the ratio $(1 - \varphi)/\varphi$ is

$$\frac{1 - \varphi}{\varphi} = \frac{h_g S_g}{h_c S_c} \tag{3}$$

Use of this equation, together with the calculated values of h_g for the blade leading-edge region and for the blade midchord region, permits the calculation of the values of Nu_c. For this purpose, the value of h_g for the vane leading-edge region was obtained from the relation for flow over a cylinder (with the diameter of the leading edge of the blade used instead of the cylinder diameter as the characteristic distance)

$$h_g = 1.14\ Re^{0.5}\ Pr^{0.4}\left(1 - \left|\frac{\theta}{90}\right|^3\right)\frac{k_g}{D} \tag{4}$$

where θ is the angle measured from the stagnation point and where $-80^\circ < \theta < 80^\circ$. For the midchord region, the flat-plate turbulent-flow correlation (with distance from the stagnation point as the characteristic distance)

$$h_g = 0.0296\ Re^{0.8}\ Pr^{1/3}\ \frac{k_g}{x} \tag{5}$$

was used.

RESULTS AND DISCUSSION

Coolant Flow Ratio as Function of Pressure Ratio

The cooling-air-inlet static pressure $p_{c,i}$ is calculated from the static pressure measured at the entrance to the rotating turbine disk corrected for friction, momentum, and rotational pressure drops between that point and the base of the blade. The turbine-inlet total pressure $P_{t,i}$ is related by a constant to the static pressure which the cooling air encounters as it exits from the blade at the engine operating design point. Thus, the ratio $p_{c,i}/P_{t,i}$ is a measure of the pressure drop through the blade. Since both the cooling air and the combustion air come from the compressor exit, the pressure ratio $p_{c,i}/P_{t,i}$ should have a practical value close to unity.

Figure 3 presents the coolant flow ratio $\dot{w}_c/\dot{w}_g$, as a function of the ratio of blade-inlet cooling-air static pressure to turbine-inlet total pressure $p_{c,i}/P_{t,i}$, for three values of cooling-air inlet temperature. The data indicate an effect of cooling-air inlet temperature. In the range of practical interest, namely a coolant flow ratio of 0.03 to 0.05, the pressure ratio varies between 0.83, at 300 K (80° F), and 1.43, at 811 K

(1000° F). Figure 3 indicates that this impingement-cooled blade may have an upper limit to the practical coolant flow ratio of 0.038 at 300 K (80° F), or 0.034 at 811 K (1000° F), or an even lower coolant flow ratio at a higher coolant temperature.

Average Midspan Temperature-Difference Ratio

Values of the average midspan temperature-difference ratio $\bar{\varphi}$ as a function of coolant flow ratio are presented in figure 4. Data for three values of turbine-inlet temperature and three values of cooling-air inlet temperature are presented. The least-squares curve fit through the data yielded the value 1.76 for the coefficient A (when $\dot{w}_c/\dot{w}_g$ is expressed in percent) and -0.604 for the exponent B in equation (1). A minor trend with change in cooling-air inlet temperature is shown. The symbols in figure 4 correspond to the symbols in table II.

Wall-Temperature Characteristics

The wall-temperature characteristics of the impingement-cooled blade are presented in figure 5 for a turbine-inlet temperature of 1644 K (2500° F) and a coolant-inlet temperature of 922 K (1200° F). These characteristics (the average, maximum, and minimum wall temperatures) are obtained from correlations of the local metal temperatures, since a cooling-air inlet temperature of 922 K (1200° F) cannot be supplied to the research engine. The figure shows the maximum blade temperature, the average blade temperature, and the minimum blade temperature as a function of coolant-to-gas flow ratio. For this blade, a coolant-to-gas flow ratio of 0.027 is sufficient to maintain the maximum wall temperature at 1255 K (1800° F) for the given turbine-inlet and coolant temperatures; the average blade temperature for these same conditions is a little less than 1200 K (1700° F). As the coolant-to-gas flow ratio is increased, the maximum, average, and minimum wall temperatures decrease. For the complete range of flow rates considered, the value of the maximum chordwise temperature difference ($T_{w,\,max} - T_{w,\,min}$) is almost constant, varying between about 117 and 125 K (210° and 225° F). For the conditions considered, figure 5 indicates that the impingement-cooled blade is cooled effectively.

Blade Potential

For a selected maximum blade-wall temperature of 1255 K (1800° F) and a cooling-air inlet temperature of 922 K (1200° F), the allowable turbine-inlet temperature was

calculated as a function of coolant-to-gas flow ratio. The allowable turbine-inlet temperature was calculated as 10/9 of the turbine relative temperature. The results shown in figure 6 were obtained by use of the φ correlation for the highest blade temperature measured (thermocouple location 9 in fig. 2). For the above conditions, a coolant-to-gas flow ratio of 0.027 was sufficient to allow operation at a turbine-inlet gas temperature of 1644 K (2500° F).

For these experimental test blades, the blade shell was made in two halves and then welded together at the leading and trailing edges. Because of the weld in the airfoil, it was believed best, from a structural standpoint, to avoid placement of thermocouples (and their attendant grooves) directly in the welded region. Since the blade hot-spot temperature is generally in the extreme leading-edge region, thermocouple location 9 probably does not represent the actual blade hot spot, and figure 6 may be a bit optimistic.

Comparison of Heat-Transfer Characteristics of Impingement-Cooled Blade with Characteristics of Other Blades

The heat-transfer characteristics of the impingement-cooled blade are compared to those of the chordwise-passage blade of reference 1 and those of the spanwise-passage blade and the simple cast blade of reference 2. The comparison was made for a coolant-inlet temperature of 922 K (1200° F) and a coolant-to-gas flow ratio of 0.05. Table III presents the comparison. The left part of the table represents the average blade wall temperature, maximum blade wall temperature, and the difference between the maximum and minimum blade wall temperatures when the turbine inlet temperature was fixed at 1644 K (2500° F). The right part of the table gives the maximum allowable turbine-inlet temperature when the blade wall has a maximum temperature of 1255 K (1800° F).

Table III clearly shows that the impingement-cooled blade is cooled more effectively than the other three blades. For the fixed turbine-inlet temperature of 1644 K (2500° F), the impingement-cooled blade has the lowest maximum wall temperature and the lowest difference between maximum and minimum wall temperatures of the four blades. Although the impingement-cooled blade has an average wall temperature higher than that of the chordwise-passage blade, the temperature distribution is more uniform, with the maximum temperature being 63 K (114° F) lower and the minimum temperature being 31 K (56° F) higher. In addition, for the fixed maximum blade temperature of 1255 K (1800° F), the impingement-cooled blade has the highest allowable turbine-inlet temperature, 1743 K (2678° F).

Comparison of Analytical and Correlated Blade Wall Temperature Distribution

The impingement-cooled blade was designed for a turbine-inlet temperature of 1644 K (2500° F), a cooling-air inlet temperature of 922 K (1200° F), and a coolant-to-gas flow ratio of 0.045. The analytical temperature distribution that resulted is shown by the solid curve in figure 7. Since a cooling-air inlet temperature of 922 K (1200° F) could not be supplied to the research engine, the blades were never operated at design conditions. In order to obtain a temperature distribution to compare with the design distribution, it was necessary to use the φ correlations for each individual location and to calculate a so-called correlated temperature distribution. This resulting distribution is shown in figure 7 by the circular data-point symbols.

The figure shows that the analytical distribution, in general, is considerably higher than the correlated distribution. On the suction surface, in particular, the difference between the two distributions is significant. This partially results from the fact that the coolant-flow split between the suction and pressure surfaces during testing was probably different from that used in the analysis. (The equations for the gas-side and coolant-side heat-transfer coefficients for the suction surface were the same as those for the pressure surface.) The correlated and analytical distributions exhibit the same general trends; both exhibit allowable differences of about 116 K (209° F) between maximum and minimum values. The analytical distribution is a conservative one, being generally higher than the correlated distribution. This might be explained in part by the fact that turbulent heat-transfer coefficients were assumed to exist along the suction and pressure midchord regions.

A more uniform chordwise temperature distribution would result if the leading-edge impingement holes were increased in size and if the suction- and pressure-surface impingement holes were decreased in size. Such modifications could minimize the overcooling of the suction and pressure surfaces and the undercooling of the leading edge shown in figure 7.

Comparison of Predicted and Experimental Coolant-Side Nusselt Numbers

Leading-edge region. - A simplified correlation was presented in reference 6 for predicting the ratio of local to average Nusselt numbers around the inside of the leading edge of a turbine blade. A correlation for the average Nusselt number was given in reference 7. By finding the product of these two correlations, evaluated at the x/L values of thermocouple positions 9 and 10, a predicted value of the local Nusselt number at a prescribed distance from the stagnation line was determined for a selected coolant flow rate and coolant temperature (coolant Reynolds number). The result, for a range

of Reynolds numbers, is shown as the line in figure 8(a). Both the Nusselt number and the Reynolds number are based on the equivalent slot width.

At the same prescribed distance from the stagnation line on both the suction and pressure surfaces as that considered above, local experimental values of the Nusselt number were determined by substituting equation (3) into the definition of the Nusselt number. The left side of equation (3) was evaluated from measured temperatures. Because of the position of the point in question, neither equation (4) nor equation (5) was used to evaluate h_g. The value that was actually used was a value on the faired part of the curve connecting the curves representing equations (4) and (5).

The resulting experimental blade-to-coolant Nusselt numbers on the suction surface are denoted by the circles and on the pressure surface by the squares in figure 8(a). The predicted local Nusselt numbers approximately represent the suction surface data. The actual location of the data points is directly related to the value selected from the faired h_g distribution, and these points could be relocated by refairing the curves representing equations (4) and (5). Nevertheless, the product of the correlations from references 6 and 7, when used in conjunction with generally accepted gas-to-blade heat-transfer coefficients, appears adequate for predicting temperatures on the leading edge of a turbine blade.

Midchord region. - Equations (3) and (5), along with the definition of the Nusselt number, were combined to obtain experimental coolant-side Nusselt numbers on the midchord suction and pressure surfaces. Predicted values of coolant-to-blade Nusselt numbers in the midchord region were obtained at the locations of the thermocouples from correlations in the literature. The correlations apply to an average value of Nusselt number for a square array of circular jets impinging onto a flat plate. The experimental Nusselt numbers were then compared with the predicted local values. The comparison is shown in figure 8(b). The correlations are from references 8 and 9 with the crossflow term in the latter set to unity (no crossflow effect).

The Nusselt number agreement between correlation of reference 8 and the suction surface data and between the correlation of reference 9 and the pressure surface data agreed favorably. On the suction surface, Nusselt numbers are presented for both thermocouple locations 7(b) and 8(a), shown in figure 2. (Thermocouples at locations 7(a) and 8(b) failed early in the test program, and so the comparison of experimental Nusselt numbers on the same blade could not be made.) The experimental Nusselt numbers for the two different suction-surface locations are nearly equal over the entire range of Reynolds numbers. These data seem to minimize the possibility of the crossflow affecting the impinging-jet heat transfer, since the experimental Nusselt numbers shown in figure 8(b) increase with increasing crossflow (increasing number of upstream jets).

Uncertainties do exist in the values of calculated wall-to-coolant Nusselt numbers based on a combination of measured temperatures and calculated gas-to-wall heat trans-

fer coefficients. However, the relative values of the Nusselt numbers should be correct, since the relative values of the heat-transfer coefficients should be correct. The location farther downstream has the higher coolant-side Nusselt number.

On the pressure surface, Nusselt numbers are presented for thermocouple locations 11(a) and 12(a). The magnitudes of the experimental Nusselt numbers at these two positions differ substantially from each other over the entire range of Reynolds numbers. As on the suction surface, the position which is farther downstream has the higher Nusselt number, contrary to what would be expected with a crossflow effect.

This lack of effect of crossflow on both the suction and pressure surfaces may be partially explained by the fact that the ratio of the flow per area of the crossflow to the flow per area of the impinging jet is less than 0.4 for even the most severe case. At least part of the large difference between the data points and the predicted values can probably be attributed to the uncertainty in the gas-to-blade heat-transfer coefficient. Also, a difference exists between the geometry of the apparatus used to establish the Nusselt number correlation and the geometry of the turbine-blade insert.

Figure 32 of reference 10 shows that the correlations from references 8 and 9 are less optimistic than the other correlations on the figure for arrays of circular jets without crossflow. Therefore, the correlations of references 8 and 9 seem to be the best of those presented in figure 32 of reference 10 for predicting average blade-to-coolant Nusselt numbers on the midchord suction and the midchord pressure surfaces, respectively.

SUMMARY OF RESULTS

An experimental investigation of an impingement-cooled turbine-rotor blade was conducted in a turbojet engine. The following results were obtained:

1. Average midspan wall temperatures for the impingement-cooled blade were successfully correlated by means of the temperature-difference ratio as a function of the coolant-to-gas flow ratio. (The temperature-difference ratio considers the effective gas temperature, the cooling-air inlet temperature to the vane, and the vane wall temperature.)

2. For a turbine-inlet temperature of 1644 K (2500° F), a coolant temperature of 922 K (1200° F), and a coolant-to-gas flow ratio of 0.027, the maximum blade temperature was calculated from correlated data to be 1255 K (1800° F). For these conditions, calculations showed that the average blade temperature was less than 1200 K (1700° F) and that the maximum chordwise blade temperature difference was 125 K (225° F).

3. The impingement-cooled blade proved to be cooled more effectively than were three convection-cooled blades tested in the same facility.

4. The coolant-side local leading-edge impingement Nusselt numbers calculated

from existing correlations agreed favorably with those determined from leading-edge experimental temperature data.

5. The coolant-side local midchord impingement Nusselt numbers calculated from existing correlations agreed favorably with those calculated from the data of the midchord region.

6. No effect of crossflow on impinging-jet heat transfer was found in the midchord region.

Lewis Research Center,
National Aeronautics and Space Administration,
Cleveland, Ohio, February 20, 1973,
501-24.

REFERENCES

1. Dengler, Robert P.; Yeh, Frederick C.; Gauntner, James W.; and Fallon, Gerald E.: Engine Investigation of an Air-Cooled Turbine Rotor Blade Incorporating Impingement-Cooled Leading Edge, Chordwise Passages, and a Slotted Trailing Edge. NASA TM X-2526, 1972.

2. Fallon, Gerald E.; and Livingood, John N. B.: Comparison of Heat-Transfer Characteristics of Two Air-Cooled Turbine Blades Tested in a Turbojet Engine. NASA TM X-2564, 1972.

3. Calvert, Howard F.; Cochran, Reeves P.; Dengler, Robert P.; Hickel, Robert O.; and Norris, James W.: Turbine Cooling Research Facility. NASA TM X-1927, 1970.

4. Crowl, Robert J.; and Gladden, Herbert J.: Methods and Procedures for Evaluating, Forming, and Installing Small-Diameter Sheathed Thermocouple Wire and Sheathed Thermocouples. NASA TM X-2377, 1971.

5. Gladden, Herbert J.; Gauntner, Daniel J.; and Livingood, John N. B.: Analysis of Heat-Transfer Tests on an Impingement-Convection- and Film-Cooled Vane in a Cascade. NASA TM X-2376, 1971.

6. Livingood, John N. B.; and Gauntner, James W.: Local Heat-Transfer Characteristics of a Row of Circular Air Jets Impinging on a Concave Semicylindrical Surface. NASA TN D-7127, 1973.

7. Chupp, Raymond E.; Helms, Harold E.; McFadden, Peter W.; and Brown, T. R.: Evaluation of Internal Heat-Transfer Coefficients for Impingement-Cooled Turbine Airfoils. J. Aircraft, vol. 6, no. 3, May-June 1969, pp. 203-208.

8. Gardon, Robert; and Cobonpue, John: Heat Transfer Between a Flat Plate and Jets of Air Impinging on It. International Developments in Heat Transfer. ASME, 1963, pp. 454-460.

9. Kercher, D. M.; and Tabakoff, W.: Heat Transfer by a Square Array of Round Air Jets Impinging Perpendicular to a Flat Surface Including the Effect of Spent Air. J. Eng. Power, vol. 92, no. 1, Jan. 1970, pp. 73-82.

10. Livingood, John N. B.; Ellerbrock, Herman H.; and Kaufman, Albert: 1971 NASA Turbine Cooling Research Status Report. NASA TM X-2384, 1971.

TABLE I. - BLADE THERMOCOUPLE LOCATIONS

Suction side					
Thermocouple location designation	Distance along span from hub section, r		Chordwise distance along surface from stagnation point, x		Ratio of chordwise distance along surface to total chordwise surface length, x/L_s (a)
	cm	in.	cm	in.	
1	1.27	0.5	4.023	1.548	0.806
2	1.27	.5	.394	.155	.079
5(a)	3.81	1.5	4.302	1.694	.862
5(b)	↓	↓	4.302	1.694	.862
6(a)			3.630	1.429	.727
6(b)			3.630	1.429	.727
7(a)			2.022	.796	.405
7(b)			2.022	.796	.405
8(a)			1.173	.462	.235
8(b)			1.173	.462	.235
9(a)			.394	.155	.079
9(b)	↓	↓	.394	.155	.079
13	5.08	2.0	3.630	1.429	.727
14	5.08	2.0	.394	.155	.079
Pressure side					
Thermocouple location designation	Distance along span from hub section, r		Chordwise distance along surface from stagnation point, x		Ratio of chordwise distance along surface to total chordwise surface length, x/L_p (b)
	cm	in.	cm	in.	
3	1.27	0.5	0.406	0.160	0.090
4	1.27	.5	3.383	1.332	.750
10(a)	3.81	1.5	.406	.160	.090
10(b)	↓	↓	.406	.160	.090
10(c)			.406	.160	.090
11(a)			1.600	.630	.355
11(b)			1.600	.630	.355
12(a)			3.028	1.192	.671
12(b)	↓	↓	3.028	1.192	.671
15	5.08	2.0	.406	.160	.090
16	5.08	2.0	3.028	1.192	.671

[a]Where L_s = 4.991 cm (1.965 in.).

[b]Where L_p = 4.511 cm (1.776 in.).

TABLE II. - SUMMARY OF ENGINE OPERATING CONDITIONS

Test series	Engine speed, rpm	Average turbine-inlet temperature, $\overline{T}_{t,i}$		Average turbine-inlet pressure, $\overline{P}_{t,i}$		Cooling-air inlet temperature, $\overline{T}_{c,i}$		Blade coolant-to-gas flow ratio, $\dot{w}_c/\dot{w}_g$, percent	Symbols used in figure 4
		K	^{o}F	N/cm^2 abs	psia	K	^{o}F		
1	7500	1367	2000	23	34	300	80	2.08 to 12.45	○
2	8300	1533	2300	25	37	300	80	2.08 to 9.54	□
3	8700	1644	2500	28	41	300	80	2.01 to 8.69	◇
4	8200	1533	2300	25	37	589	600	2.10 to 8.78	▽
5	8700	1644	2500	28	41	589	600	4.13 to 8.18	◹
6	7500	1367	2000	22	32	811	1000	3.23 to 9.00	◹

TABLE III. - COMPARISON OF HEAT-TRANSFER CHARACTERISTICS OF FOUR BLADES

[Coolant inlet temperature, $T_{c,i}$, 922 K (1200^{o} F); coolant-to-gas flow ratio, $\dot{w}_c/\dot{w}_g$, 0.05.]

Blade configuration	Average blade wall temperature, $\overline{T}_w$		Maximum blade wall temperature, $T_{w,max}$		Maximum chordwise blade wall temperature difference, $T_{w,max} - T_{w,min}$		Turbine-inlet temperature, $\overline{T}_{t,i}$	
	K	^{o}F	K	^{o}F	K	^{o}R	K	^{o}F
	Turbine-inlet gas temperature, $T_{t,i}$, 1644 K (2500^{o} F)						Maximum blade wall temperature, $T_{w,max}$, 1244 K (1800^{o} F)	
Impingement	1154	1618	1208	1715	124	223	1743	2678
Chordwise passage (ref. 1)	1129	1573	1272	1829	218	393	1613	2444
Spanwise passage (ref. 2)	1158	1624	1244	1780	166	299	1663	2534
Simple cast (ref. 2)	1229	1753	1309	1897	166	298	1556	2341

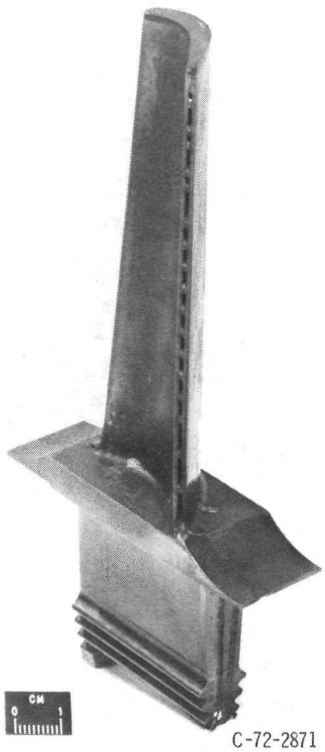

C-72-2871

(a) View of slotted trailing edge.

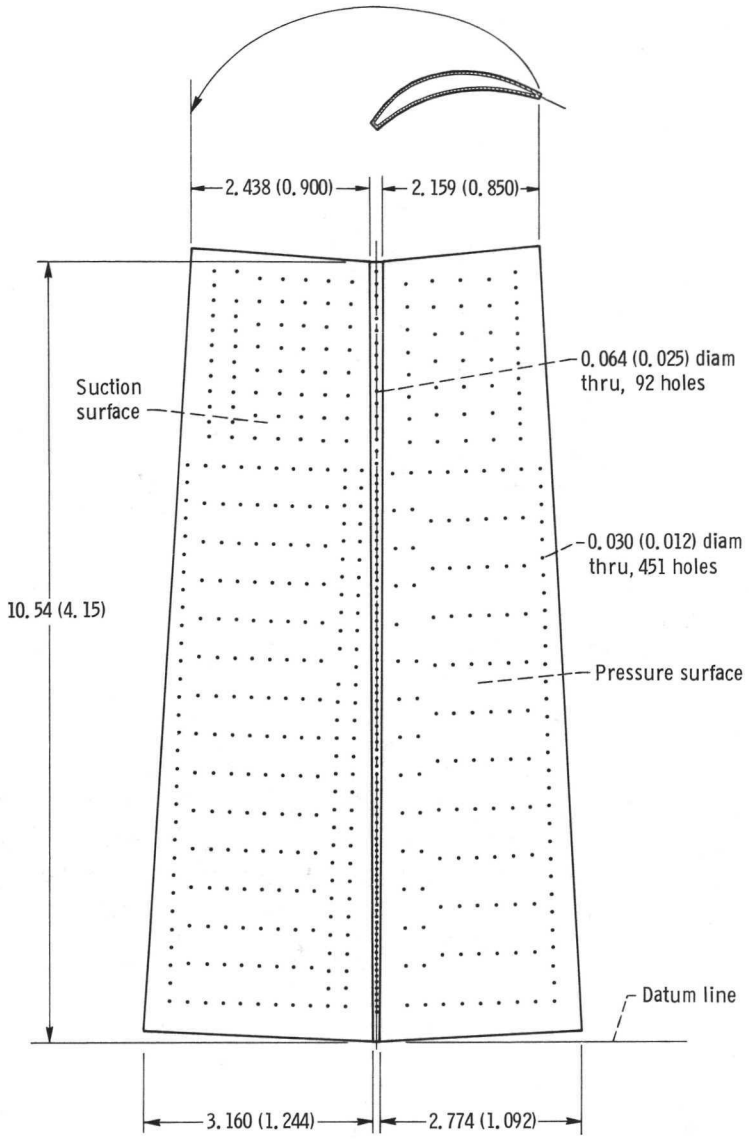

(b) Developed view of insert showing leading-edge and midchord hole locations. (Dimensions in cm (in.).)

Figure 1. - Impingement-cooled blade.

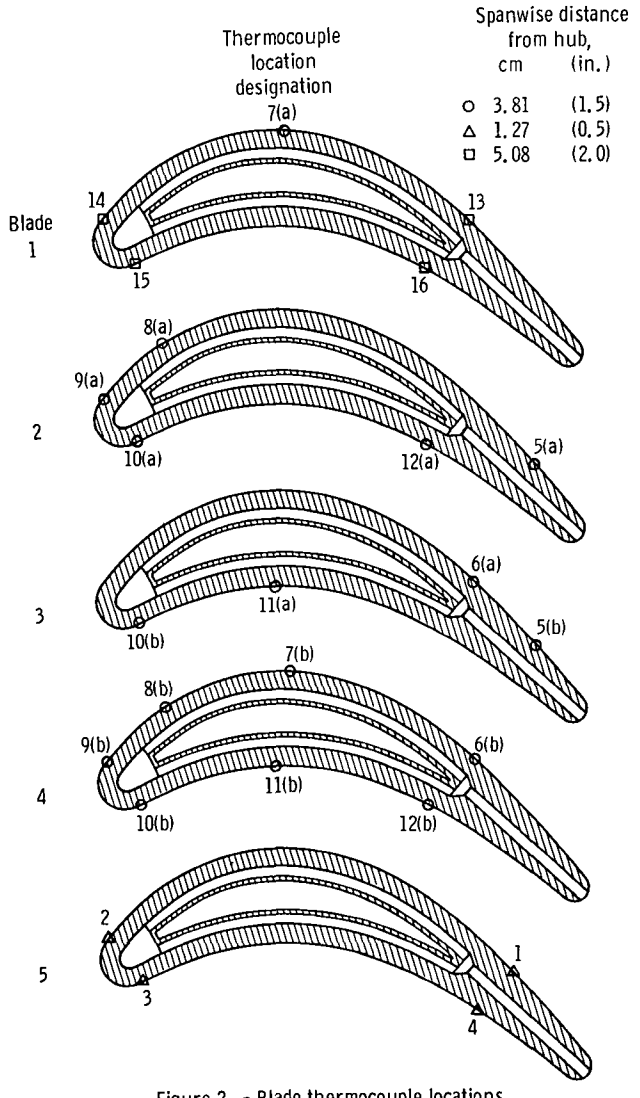

Figure 2. - Blade thermocouple locations.

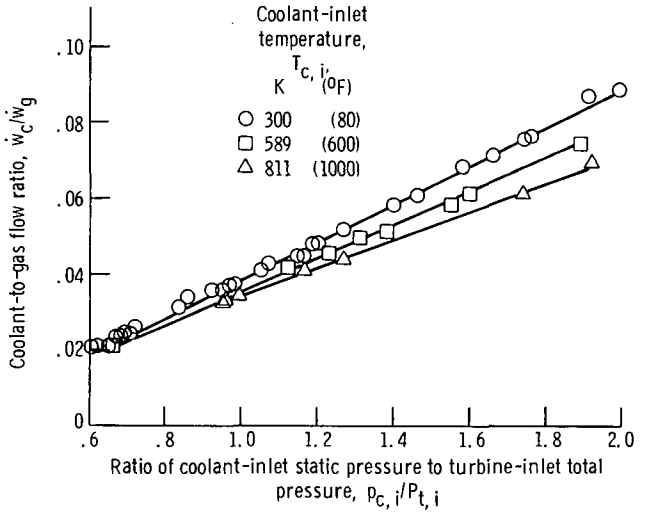

Figure 3. - Coolant flow ratio through the blade as a function of pressure ratio for various coolant-inlet temperatures.

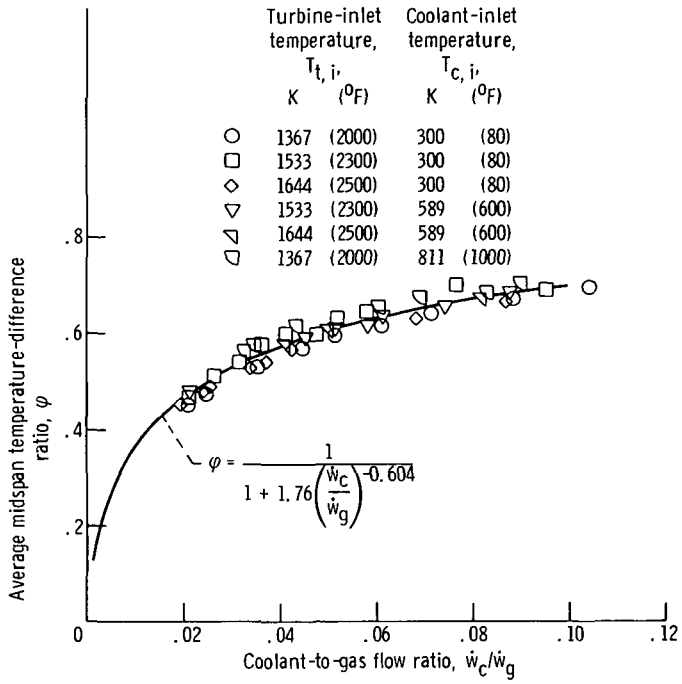

Figure 4. - Average midspan temperature-difference ratio as function of coolant-to-gas flow ratio for impingement-cooled turbine blade.

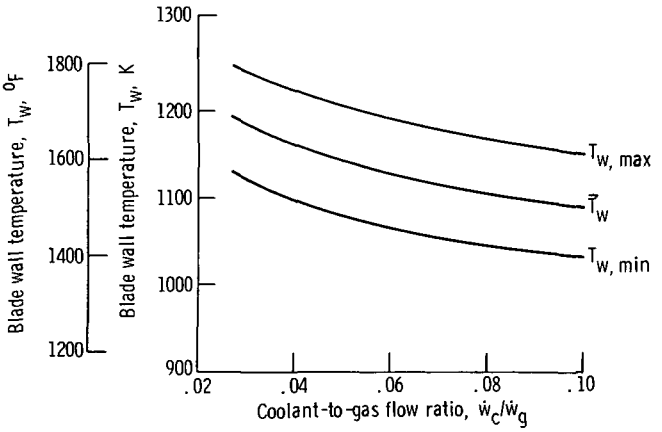

Figure 5. - Blade wall-temperature characteristics at the midspan of impingement-cooled blade. Turbine-inlet temperature, 1644 K (2500° F); coolant-inlet temperature, 922 K (1200° F).

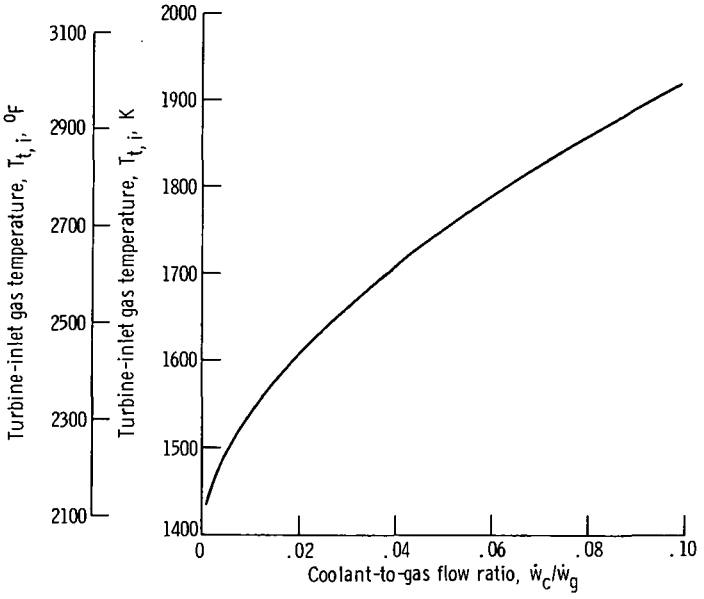

Figure 6. - Potential stator-inlet total gas temperature as a function of coolant flow ratio. Maximum blade-wall temperature, 1255 K (1800° F); coolant-inlet temperature, 922 K (1200° F).

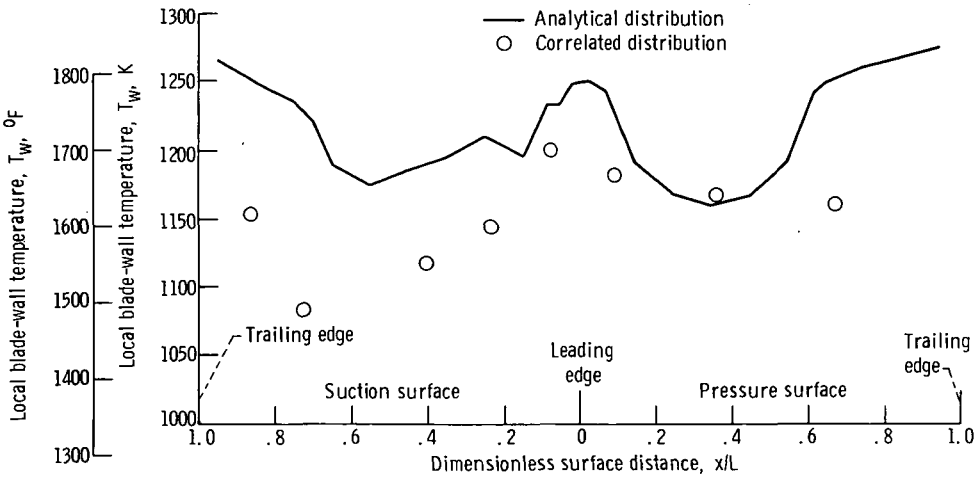

Figure 7. - Comparison of analytical and correlated chordwise blade-wall temperature distribution at spanwise distance of 3.81 centimeters (1.5 in.) from hub section. Turbine-inlet temperature, 1644 K (2500° F); relative turbine-inlet temperature 1480 K (2204° F); coolant-inlet temperature, 922 K (1200° F); coolant-to-gas flow ratio, 0.045.

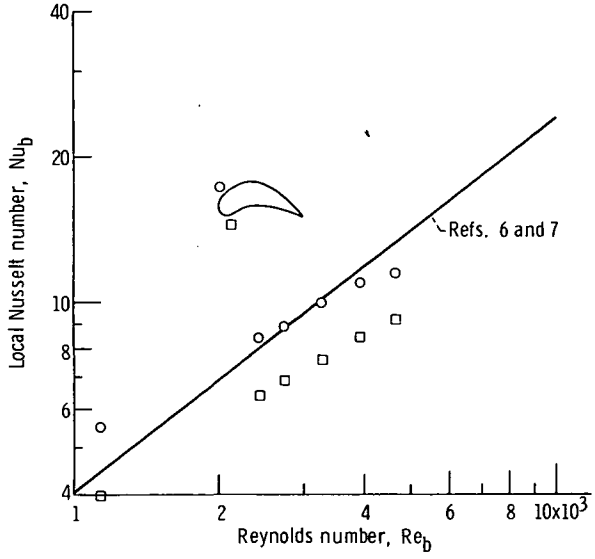

(a) Leading-edge region.

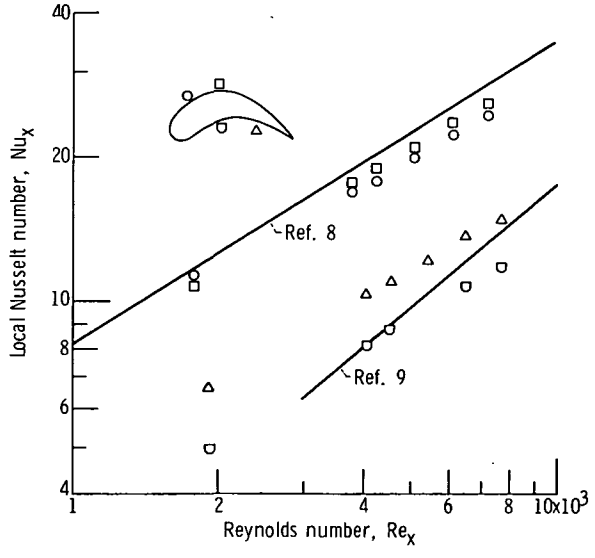

(b) Midchord region.

Figure 8. - Comparison of experimental and analytical local impingement Nusselt numbers. Turbine-inlet temperature, 1533 K (2300^0 F); coolant inlet temperature, 589 K (600^0 F).

Page Intentionally Left Blank

NATIONAL AERONAUTICS AND SPACE ADMINISTRATION
WASHINGTON, D.C. 20546

OFFICIAL BUSINESS
PENALTY FOR PRIVATE USE $300

SPECIAL FOURTH-CLASS RATE BOOK

POSTAGE AND FEES PAID
NATIONAL AERONAUTICS AND SPACE ADMINISTRATION
451

U.S.MAIL

POSTMASTER: If Undeliverable (Section 158 Postal Manual) Do Not Return

"The aeronautical and space activities of the United States shall be conducted so as to contribute . . . to the expansion of human knowledge of phenomena in the atmosphere and space. The Administration shall provide for the widest practicable and appropriate dissemination of information concerning its activities and the results thereof."

—NATIONAL AERONAUTICS AND SPACE ACT OF 1958

NASA SCIENTIFIC AND TECHNICAL PUBLICATIONS

TECHNICAL REPORTS: Scientific and technical information considered important, complete, and a lasting contribution to existing knowledge.

TECHNICAL NOTES: Information less broad in scope but nevertheless of importance as a contribution to existing knowledge.

TECHNICAL MEMORANDUMS: Information receiving limited distribution because of preliminary data, security classification, or other reasons. Also includes conference proceedings with either limited or unlimited distribution.

CONTRACTOR REPORTS: Scientific and technical information generated under a NASA contract or grant and considered an important contribution to existing knowledge.

TECHNICAL TRANSLATIONS: Information published in a foreign language considered to merit NASA distribution in English.

SPECIAL PUBLICATIONS: Information derived from or of value to NASA activities. Publications include final reports of major projects, monographs, data compilations, handbooks, sourcebooks, and special bibliographies.

TECHNOLOGY UTILIZATION PUBLICATIONS: Information on technology used by NASA that may be of particular interest in commercial and other non-aerospace applications. Publications include Tech Briefs, Technology Utilization Reports and Technology Surveys.

Details on the availability of these publications may be obtained from:

SCIENTIFIC AND TECHNICAL INFORMATION OFFICE

NATIONAL AERONAUTICS AND SPACE ADMINISTRATION

Washington, D.C. 20546